

Making Generated Images Hard To Spot: A Transferable Attack On Synthetic Image Detectors

Xinwei Zhao

Department of Electrical and Computer Engineering
Drexel University
Philadelphia, PA, 19104, USA
Email: xz355@drexel.edu

Matthew C. Stamm

Department of Electrical and Computer Engineering
Drexel University
Philadelphia, PA, 19104, USA
Email: mcs382@drexel.edu

Abstract—Visually realistic GAN-generated images have recently emerged as an important misinformation threat. Research has shown that these synthetic images contain forensic traces that are readily identifiable by forensic detectors. Unfortunately, these detectors are built upon neural networks, which are vulnerable to recently developed adversarial attacks. In this paper, we propose a new anti-forensic attack capable of fooling GAN-generated image detectors. Our attack uses an adversarially trained generator to synthesize traces that these detectors associate with real images. Furthermore, we propose a technique to train our attack so that it can achieve transferability, i.e. it can fool unknown CNNs that it was not explicitly trained against. We evaluate our attack through an extensive set of experiments, where we show that our attack can fool eight state-of-the-art detection CNNs with synthetic images created using seven different GANs, and outperform other alternative attacks.

I. INTRODUCTION

Recent technological advances have enabled the creation of synthetic images that are visually realistic. Generative adversarial networks (GANs) [1] in particular have driven this development. Several GANs have been proposed that are capable of synthetically generating images of both objects and human faces that are convincingly real to human observers [2], [3], [4], [5], [6], [7], [8]. Unfortunately, these synthetic image generation techniques can be used for malicious purposes, such as the creation of fake personas to be used as part of misinformation campaigns.

To combat this threat, researchers have developed many techniques to detect GAN-generated images [9], [10], [11], [12], [13] and to attribute them to the specific GAN used to create them [14], [15], [16]. At the same time, adversarial examples have arisen as a new threat to classifiers built from neural networks [17], [18], [19], [20], [21], [22]. These represent important threats to the forensic community because they can be used as an anti-forensic attack against forensic detectors [23], [24], [25]. Recent work from the forensic community, however, suggests that these attacks may not achieve transferability, i.e. they may be unable to attack classifiers other than those they were directly trained against [26], [27].

For an anti-forensic attack to be successful, it must (1) fool a victim classifier and (2) maintain high visual quality within the attacked image. Furthermore, it is highly desirable for an attack to (3) transfer to victim classifiers not seen during

training and (4) be easily deployable in practical scenarios, i.e. it should work on images of any size, not require specific knowledge of the image window analyzed by a forensic CNN, deploy quickly and efficiently, etc.

In this paper, we propose a new attack that is capable of fooling forensic synthetic image detectors into thinking that GAN-generated images are in fact real images. This attack achieves each of the four goals described above, including a significant degree of transferability, which enables it to attack victim classifiers that are unseen during training. Instead of crafting adversarial examples that exploit flaws in forensic detectors, our attack uses an anti-forensic generator to synthesize forensic traces associated with real images. We propose GAN-based approaches for training our anti-forensic generator for both white-box scenarios and zero-knowledge scenarios. Once the anti-forensic generator is trained, it can be used to attack images of arbitrary size without requiring re-training or additional tuning to the image under attack.

The main contributions of this work are as follows:

- We propose a new generative anti-forensic attack that is able to fool CNN-based synthetic image detectors. Our attack operates by synthesizing forensic traces associated with real images while introducing no perceptible distortions into an attacked image.
- We propose an ensemble loss training strategy that enables our attack to achieve transferability in zero-knowledge scenarios.
- We demonstrate the effectiveness of our attack against many state-of-the-art forensic CNNs, using synthetic images from a wide variety of different GANs.
- We show that our proposed attack achieves in a higher attack success rate, image quality, and transferability than other alternative attacks, including other adversarial example and GAN-based attacks.

II. RELATED WORK

Here we briefly review related work on detecting GAN-generated images and adversarial attacks.

GAN-Generated Image Detectors: To defend against the misinformation threat posed by synthetic media, significant research has been done to create GAN-generated image detection algorithms [16], [28], [9], [10], [11], [12], [13]. Previous

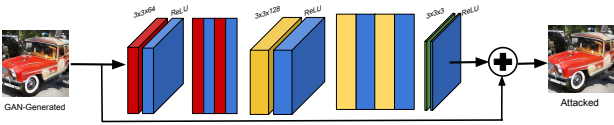


Fig. 1. Architecture of the proposed anti-forensic generator.

research has shown that GANs leave behind forensic traces that are distinguishable from real images. These forensic traces left by GANs can be utilized to detect GAN-generated images. Some approaches operate in a data driven manner [28], [13], [9], while other approaches utilize semantic information [10] or hand-crafted features [11]. Additionally, forensic techniques are also developed to identify which GAN was used to generate an image [14], [16], [12].

Adversarial Attacks on Forensic Classifiers: At the same time, adversarial attacks on neural networks have emerged as an important threat [18], [29]. These attacks can be adapted to attack forensic classifiers [23]. Roughly speaking, we can group these attacks into two different families: adversarial-example-based attacks and GAN-based attacks.

Adversarial example attacks operate by creating additive image perturbations that cause a victim classifier to misclassify the image. Several techniques have been proposed to create these perturbations, including L-BFGS [17], FGSM and iterative-FG [18], [19], JSMA [20], CW [21], PGD [22]. Attacks based on adversarial examples have been used to forensic algorithms, including camera model identification algorithms [25] and deepfake detectors [24]. Research by Barni et. al has shown, however, that adversarial example attacks do not transfer well to other forensic classifiers [26].

Previous research has also shown that GANs can be utilized to construct attacks that falsify forensic traces. GANs were used by Chen et al. to falsify camera model fingerprints [30] and by Cozzolino et al. to falsify device fingerprints [31]. Kim et. al used a GAN to remove forensic traces left by median filtering [32]. However, research has shown that the GAN-based anti-forensic attacks also have trouble in transferring [27].

III. PROPOSED ATTACK

Our attack is designed to modify a GAN-generated image I so that a forensic CNN will instead classify it as a ‘real’ image. This forensic CNN is alternately referred to as the victim classifier, and is trained to differentiate between real and GAN-generated images.

Our attack operates by passing the GAN-generated image through a pre-trained anti-forensic generator G in order to falsify its forensic traces. The anti-forensic generator is designed to remove forensic traces associated with GAN-generated images and synthesize traces associated with ‘real’ images. As a result, a victim classifier will classify the attacked GAN-generated image $G(I)$ as a real one. Furthermore, the anti-forensic generator designed to make no changes to the image’s contents and to introduce no visually perceptible distortions into the attacked image. This will prevent a human from visually identifying that an image was attacked.

The anti-forensic generator in our attack learns to synthesize ‘real’ forensic traces through adversarial training. It is trained as part of a GAN in which the discriminator is replaced by a forensic classifier (or set of classifiers) that has been pre-trained to learn the distribution of forensic features associated with real and GAN-generated images.

Different strategies are used to train the anti-forensic generator depending on whether the attack is launched in a white-box or zero-knowledge scenario. In the white-box scenario, our attack aims to synthesize forensic features with the distribution learned by the victim classifier, even if they deviate from the ideal feature distribution of real images. In the zero-knowledge scenario, our attack aims to learn the distribution of forensic features of real images. However it avoids synthesizing features in regions where different classifiers may make different decisions. Instead, it aims to synthesize features that any classifier will likely associate with a real image.

A. Proposed Anti-Forensic Generator Architecture

The proposed anti-forensic generator consists of a sequence of convolutional layers followed by ReLU activations [33] shown in Figure 1. The first three convolutional layers use 64 filters, the middle three convolutional layers use 128 filters, and the final convolutional layer uses three filters to reduce the 128 feature maps to a three color channel image. The output of the generator is the summation of the input of the generator and the output of the last activated convolutional layer. The skip connection is designed to give the generator a better initialization for producing high visual quality attacked images. All convolutional layers use 3×3 filter with stride 1. The small filter size allows the generator to synthesize forensic traces in small areas. We avoid using any pooling layers to ensure that the output of the generator is of the same size as the input of the generator. Therefore, the proposed anti-forensic generator can be applied to images of arbitrary sizes, and does not need to be trained for images of different sizes individually. This characteristic makes the deployment of the proposed anti-forensic generator efficient and quick.

B. Anti-Forensic Generator Training

When adversarially training the anti-forensic generator G , we formulate a loss function to ensure that a attacked image can both fool a victim classifier and maintain high visual quality. This loss function \mathcal{L}_G consists of the weighted sum of two terms: the perceptual loss \mathcal{L}_p and classification loss \mathcal{L}_c

$$\mathcal{L}_G = \alpha \mathcal{L}_p + \mathcal{L}_c \quad (1)$$

where α is used to balance the trade-off between the visual quality and performance of the attack.

Perceptual Loss: This term is used to minimize distortions introduced by the anti-forensic generator and control the visual quality of the attacked image. We define this term as the mean absolute difference between the GAN-generated image I (i.e the input of the generator) and the attacked image produced by the generator $G(I)$, such that

$$\mathcal{L}_p = \frac{1}{N} \|I - G(I)\|_1 \quad (2)$$

where N is the number of pixels in I and $G(I)$.

Classification Loss: This term is used to measure if the attacked images produced by the anti-forensic generator can fool the CNN detector used for training. It allows the generator to learn forensic traces learned by the CNN detector. The classification loss is provided by the victim classifier for white-box attacks, and is provided by an ensemble of classifiers chosen by the attacker for zero-knowledge attacks.

White-Box Attack Training: In the white-box scenario, the attacker has direct access to the forensic CNN under attack. Hence, the anti-forensic generator can be directly trained against the victim classifier. In this case, we define the classification loss \mathcal{L}_c as the softmax cross-entropy between the CNN detector’s output of attacked images and the real class,

$$\mathcal{L}_c = - \sum_k t_k \log (C(G(I))_k), \quad (3)$$

where $C(\cdot)$ is the victim classifier and t_k is the k^{th} entry of ideal softmax vector with a 1 for the real class and a 0 for the fake class. Defining the classification loss in this manner incentivizes the anti-forensic generator to learn the victim classifier’s model of forensic features from real images.

Zero-Knowledge Attack Training: In the zero-knowledge scenario, the attacker has no access to the victim classifier that they wish to attack, nor do they know its architecture. This differs from the black box scenario in which the attacker can probe the victim classifier through an API, then observe the victim classifier’s input-output relationship. Instead, the attacker must rely entirely on the transferability of their attack to fool the victim CNN.

To achieve transferability, we propose adversarially training against an ensemble of forensic classifiers created by the attacker. Here, the classification loss \mathcal{L}_c is formulated as the weights sum of individual classification loss pertaining to each CNN detector in the ensemble,

$$\mathcal{L}_c = \sum_{s=1}^S \beta^{(s)} \mathcal{L}_c^{(s)}, \quad (4)$$

where S is the number of CNN detectors in the ensemble, $\mathcal{L}_c^{(s)}$ corresponds to individual classification loss of the s^{th} CNN detector calculated using Equation 3, $\beta^{(s)}$ corresponds to the weight of s^{th} individual classification loss.

Each classifier in the ensemble learns to partition the forensic feature space into separate regions for real and GAN-generated images. By defining the classifier loss in this fashion, we incentivize the anti-forensic generator to synthesize forensic features that lie in the intersection of these regions. If a diverse set of classifiers are used to form the ensemble, this intersection will likely lie inside the decision region that other classifiers associate with real images.

IV. EXPERIMENTAL SETUP

A. Datasets

We created two datasets to evaluate our attacks, each containing both real and GAN-generated images. The first

dataset contains only images of human faces, while the second contains images of non-human objects.

Human Face Dataset: This dataset consists of real images and GAN-generated images of human faces. The GAN-generated images were created using StyleGAN [4], StyleGAN2 [3], and StarGAN-v2 [2]. StyleGAN and StyleGAN2 generated images were downloaded from publicly available datasets shared by Nvidia Research Lab [34], [35]. The StarGAN-v2 generated images were created using pre-trained StarGAN-v2 generator shared at [36]. The real images were downloaded from FFHQ dataset [3] and CelebA-HQ dataset [7]. In total, the human face dataset contains 66,000 real images with 44,000 from FFHQ and 22,000 from CelebA-HQ; 126,000 GAN-generated images drawn equally from StyleGAN, StyleGAN2, and StarGAN-v2.

Next, we partitioned the data into two disjoint training sets, the *D-set* and the *A-set*, as well as an evaluation set *Eval-set*. The *D-set* was used to train the victim forensic CNN detectors. It contains 60,000 GAN-generated images drawn equally from StyleGAN, StyleGAN2 and StarGAN-v2; and 60,000 real images with 40,000 from FFHQ and 20,000 from CelebA-HQ. The *A-set* was used to train the proposed attack. Since training the proposed attack only requires GAN-generated images, *A-set* contains 60,000 GAN-generated images drawn equally from StyleGAN, StyleGAN2 and StarGAN-v2.

We benchmarked the baseline performance of the victim forensic CNN detectors and evaluated the performance of our proposed attack against these CNNs using a common evaluation set, *Eval-set*. The *Eval-set* contains 6,000 GAN-generated images drawn equally from StyleGAN, StyleGAN2 and StarGAN-v2; and 6,000 real images with 4,000 from FFHQ and 2,000 from CelebA-HQ.

Object Dataset: This dataset contains real images and GAN-generated images of objects. The object dataset is a subset of publicly available ForenSynths dataset [13]. The ForenSynths dataset was created to demonstrate that CNNs could learn general forensic traces of synthesized images. Therefore CNNs trained on generated images produced by one GAN method can detect generated images produced by other generative models. The training set of ForenSynths dataset contains only ProGAN generated images of objects and real images from LSUN dataset [37]. The testing set of ForenSynths dataset contains varying numbers of generated images produced by different generative methods.

From the training set of the ForenSynths dataset, we created two disjoint training sets: *D-set* for training victim CNN detectors and *A-set* for training the proposed attack. *D-set* contains 50,000 randomly selected ProGAN generated images and 50,000 randomly selected real images. *A-set* contains 50,000 randomly selected ProGAN generated images.

We benchmarked the baseline performance of victim forensic CNN detectors and evaluated the performance of our proposed attack against these CNNs using a common evaluation set, *Eval-set*. *Eval-set* contains 4,000 real images from LSUN, and all the generated images of objects created by six

TABLE I
CLASSIFICATION ACCURACIES OF VICTIM CNN DETECTORS ACHIEVED
ON THE HUMAN FACE DATASET AND THE OBJECT DATASET.

CNNs	Human Face Dataset	Object Dataset
Xception	99.67%	99.75%
ResNet-50	78.26%	99.14%
DenseNet	96.39%	97.04%
MISLNet	99.93%	99.15%
PHNet	95.15%	99.73%
SRNet	99.50%	99.78%
Image CNN	99.49%	99.10%
CamID CNN	99.16%	99.46%
Avg.	95.94%	99.14%

different GAN methods from the testing set of ForenSynths dataset, which consists of 26,300 images comprised of 4,000 images from ProGAN [7], 1,300 from CycleGAN [38], 6,000 from StyleGAN [4], 8,000 from StyleGAN2 [3], 2,000 from BigGAN [5], and 5,000 from GauGAN [6].

B. Victim Forensic CNN Detectors

Before training and evaluating the proposed attack, we trained and benchmarked the performance of forensic CNNs on detecting GAN-generated images. These forensic CNNs were trained as binary classifiers to differentiate between real images and GAN-generated images. We used eight state-of-the-art CNN models trained as GAN-generated image detectors, Xception [39], ResNet-50 [40], DenseNet [41], MISLNet [42], PHNet [43], SRNet [44], Image CNN [45], and CamID CNN [46]. We trained each forensic CNN individually using the *D-set* of the human face dataset and the object dataset. This yielded 16 CNN detectors in total and formed the set of victim classifiers we attacked in this paper.

The classification accuracies of victim CNN detectors on both datasets are shown in Table I. On average, the average classification accuracy is 95.94% on the human face dataset and 99.14% on the object dataset.

C. White-Box Attack

The first set of experiments was designed to evaluate the effectiveness of our proposed attack in the white-box scenario. Here, we assume the attacker has access to the victim classifier and can train directly against it.

For each victim CNN detector trained on the human face dataset and the object dataset, we trained an individual anti-forensic generator to attack it. To evaluate the performance of the anti-forensic generator, we used the generator to attack each GAN-generated image in the *Eval-set*, saving the attacked images to disk as PNG files. This is to ensure the pixel values of attacked images reside in the range from 0 to 255. Next, we calculated the attack success rate by using the victim CNN detector to classify the attacked images. To evaluate the visual quality of attacked images, we calculated the mean PSNR between the GAN-generated images and the attacked images.

The anti-forensic generators presented in this paper were trained from scratch for 32 epochs with a learning rate of 0.0001. Weights were initialized using Xavier initializer [47] and biases were initialized as 0's, and were optimized using

stochastic gradient descent. To balance the image quality and attack success rates, α in equation 1 was chosen after a grid search range from 1 to 200 with an increment of 20. As a result, α equals to 20 for attacks on the human face dataset and 100 for attacks on the object dataset.

D. Zero-Knowledge Attack

This set of experiments was conducted to evaluate the proposed attack in the zero-knowledge scenario. We assume the attacker has no knowledge about the victim CNN detector that the investigator would use to classify images. Particularly, the attacker has no access to the victim CNN detector and cannot observe any input or output of the CNN detector, since the investigator may use a private CNN detector that the attacker by all means cannot have access to. This is a more realistic yet challenging scenario. In the zero-knowledge scenario, we evaluated the transferability of the proposed attack to attack unseen CNN detectors.

To achieve the transferability, we built an ensemble of forensic CNN detectors to train the proposed anti-forensic generator. To mimic the zero-knowledge scenario, each ensemble used to train the attack did not include the victim classifier. We assume that if the attacker has no knowledge of the victim classifier's architecture, the attacker will use all available CNNs in their ensemble to strengthen their attack. Due to limited GPU memory, Xception was excluded from the training ensemble in our experiments. We trained zero-knowledge attacks using same hyperparameters and other settings as white-box attacks.

V. EXPERIMENTAL RESULTS AND DISCUSSION

A. White-Box Attack Results

Table II shows the performance achieved by white-box attacks on both datasets. Results are presented for our proposed attack, as well as other existing GAN-based and adversarial example based attacks. Here, the attack success rate (ASR) corresponds to the mean ASR achieved over synthetic images from all GAN generators for a particular victim CNN. Similarly, the PSNR in this table is defined as the mean PSNR between the original and attacked image.

Proposed Attack Performance: The performance of our proposed attack is shown along the rightmost columns of Table II. On average, our proposed attack achieved an attack success rate of 93.66% against detectors trained on the Human Face Dataset while maintaining an average PSNR of 48.95. Similarly, our proposed attack achieved an ASR of 91.62% against detectors trained on the Object dataset while maintaining an average PSNR of 53.21. Example images created by the proposed attack are shown in Figure 2. From this figure, we can see that our attack introduces no visually identifiable artifacts.

These results indicate that our attack can successfully fool a wide variety of CNNs with different architectures trained to detect synthetic images. In each case, our attack maintained a very high image quality, indicating that our attack is not detectable to the human eye. Additionally, these results show that our attack can make synthetic images created by a wide

TABLE II
MEAN ATTACK SUCCESS RATES AND MEAN IMAGE QUALITY ACHIEVED FOR WHITE-BOX ATTACKS.

Human Face Dataset												
	Residual Gen. [32]		MISLGAN [30]		CW [21]		FGSM [18]		PGD [22]		Proposed	
CNNs	ASR%	PSNR	ASR%	PSNR	ASR%	PSNR	ASR%	PSNR	ASR%	PSNR	ASR%	PSNR
Xception	98.43	29.01	66.68	32.24	98.48	47.29	54.17	44.20	100.00	47.32	100.00	45.52
ResNet-50	42.73	28.82	66.05	34.64	40.91	38.78	37.50	40.01	57.20	35.13	81.23	35.97
DenseNet	99.37	29.72	99.97	35.11	94.32	50.36	87.50	44.16	98.86	51.31	97.08	54.28
MISLNet	98.18	29.82	97.93	34.50	95.46	50.53	52.65	44.26	100.00	51.17	99.40	51.28
PHNet	96.83	30.21	99.68	34.84	98.86	51.05	97.73	51.14	99.24	51.22	94.94	41.85
SRNet	97.53	29.46	94.28	33.09	95.83	49.84	81.87	51.14	100.00	51.22	88.05	50.97
ImageCNN	66.67	29.21	80.50	34.36	100.00	49.54	0.00	44.47	94.70	49.04	94.31	53.64
CamID CNN	99.80	28.89	42.23	33.30	94.69	49.25	0.38	44.16	92.88	51.15	94.25	58.10
Avg.	87.44	29.39	80.92	34.01	89.82	48.33	51.47	45.44	92.86	48.44	93.66	48.95

Object Dataset												
	Residual Gen.		MISLGAN		CW		FGSM		PGD		Proposed	
CNNs	ASR%	PSNR	ASR%	PSNR	ASR%	PSNR	ASR%	PSNR	ASR%	PSNR	ASR%	PSNR
Xception	99.63	39.73	94.83	32.09	66.67	50.31	74.82	51.19	67.42	51.15	99.52	52.59
ResNet-50	94.61	38.51	88.46	31.50	89.85	49.58	74.79	51.16	86.36	51.17	95.24	55.41
DenseNet	95.22	37.52	95.15	31.22	81.23	50.80	79.93	51.15	81.81	51.16	91.16	50.22
MISLNet	83.53	40.49	99.12	31.75	64.02	51.08	65.91	51.26	71.21	51.16	92.70	50.97
PHNet	96.46	40.22	83.07	31.00	82.20	50.93	81.82	51.15	83.71	51.15	98.02	51.99
SRNet	82.06	37.36	94.06	31.68	61.35	46.61	0.00	51.16	72.35	51.15	82.87	56.41
ImageCNN	63.42	38.66	81.09	33.43	67.05	50.95	69.70	51.46	69.32	51.15	80.57	55.32
CamID CNN	80.39	39.02	75.69	31.37	60.61	49.01	59.09	51.34	57.20	51.15	93.05	52.77
Avg.	86.95	38.94	88.93	31.76	71.62	49.91	63.19	51.23	73.67	51.16	91.64	53.21

TABLE III
MEAN ATTACK SUCCESS RATES AND MEAN IMAGE QUALITY ACHIEVED FOR ZERO-KNOWLEDGE ATTACKS.

	Human Face Dataset						Object Dataset									
	CW		FGSM		PGD		Proposed		CW		FGSM		PGD		Proposed	
CNNs	ASR%	PSNR	ASR%	PSNR	ASR%	PSNR	ASR%	PSNR	ASR%	PSNR	ASR%	PSNR	ASR%	PSNR	ASR%	PSNR
Xception	19.75	39.58	17.58	40.07	0.54	38.89	91.07	37.93	45.70	40.95	41.67	40.12	82.19	39.06	96.63	39.95
ResNet-50	19.53	39.99	20.18	40.07	18.13	38.15	24.35	42.90	70.20	41.09	50.43	40.13	54.60	39.06	80.45	41.75
DenseNet	12.72	39.97	4.06	40.07	4.87	38.92	87.30	38.79	68.74	41.17	52.71	40.13	60.87	38.34	95.19	40.46
MISLNet	0.50	39.91	0.00	40.06	0.05	38.89	39.80	38.14	43.37	41.63	52.92	40.11	64.88	39.06	25.04	41.39
PHNet	4.22	40.18	0.08	40.07	14.61	38.98	91.62	41.69	51.46	41.38	41.67	40.13	52.16	39.09	97.48	42.18
SRNet	11.91	39.72	16.45	40.07	1.08	38.98	88.78	40.16	11.73	41.25	16.45	40.13	0.00	39.09	8.49	39.95
ImageCNN	11.09	39.55	11.69	40.03	14.77	38.87	86.73	41.27	39.34	41.20	52.97	40.02	75.92	39.06	60.38	41.03
CamID CNN	0.05	39.84	0.00	40.07	10.82	38.92	91.17	42.77	52.70	40.82	53.57	40.09	85.15	39.13	99.06	43.43
Avg.	9.97	39.84	8.85	40.06	6.47	38.84	75.10	40.46	52.70	41.19	45.30	40.11	59.75	38.99	70.30	41.27

variety of GANs appear to be real. We note that for attacks on the object dataset, our proposed attack was trained using only ProGAN generated images. Despite this, our attack can still reliably fool all detectors used in this experiment. These results show that our attack can be used on synthetic images made by GANs that our attack was not explicitly trained with.

Finally, we note that our proposed attack outperforms all other adversarial and GAN-based attacks. These results were significantly more pronounced on the Object Dataset, where our attack achieved an ASR that was 17% higher than then best performing adversarial example attack (PGD). These results are discussed in greater detail below.

Comparison With Adversarial Example Attacks: We compared our proposed attack with three well-known adversarial example attacks: Carlini-Wagner (CW) [21], Fast Gradient Sign Method (FGSM) [18], and Projected Gradient Descent (PGD) [22]. We used the CleverHans toolbox [48] to launch these attacks, then saved attacked images as PNGs. We note that due to computational limitations, adversarial example attacks were evaluated using a representative subset of the *Eval-set*. This is because adversarial example attacks must be individually trained for each image that they attack. For these experiments, our *Eval-set* for each adversarial example attack corresponded to 6,240 images for the Human

Face Dataset and 12,480 images for the Object Dataset.

From Table II, we can see that at the same image quality our attack outperformed adversarial example attacks. On the Human Face Dataset, our attack achieved an attack success rate of 93.66%. By contrast, the CW attack achieved an ASR of 89.82%, FGSM achieved an ASR of 51.47%, and PGD achieved an ASR of 92.86%. These results were more pronounced on the Object Dataset. Our attack achieved an average ASR of 91.64%, while CW achieved an ASR of 71.62%, FGSM achieved an ASR of 63.19%, and PGD achieved an ASR of 73.67%. These results show that even in white-box scenarios, our attack yields important performance advantages over adversarial example attacks.

We note that in these experiments, we chose the parameters for each adversarial example attack such that the mean PSNRs of attacked images were similar to those obtained by our attack. This was done for two reasons. The first was to maintain a fair comparison between our attack and these attacks. The second was to maintain acceptable visual quality for anti-forensic applications. It is well-known that a stronger attack typically means more visible perturbations. While this can be acceptable in computer vision algorithms, it is not acceptable for anti-forensic applications. Images with implausible visual distortions such as speckles will be rejected as inauthentic by

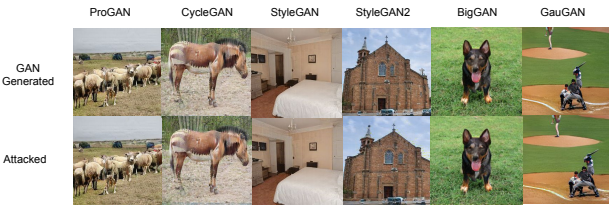


Fig. 2. Attacked images produced by the proposed white-box attack.

humans. As a result, anti-forensic attacks have a higher visual quality requirement.

Comparison With Other Anti-Forensic Generators: We also compared our proposed attack to existing GAN-based anti-forensic attacks [32], [30]. The results in Table II show that our proposed attack can outperform these attacks in terms of both ASR and image quality. On the Human Face Dataset, our attack generator achieved an ASR that was 6.22% than the residual generator [32] and 12.74% higher than MISL-GAN [30] while maintaining at least 15dB PSNR higher in image quality. We note that the image qualities achieved by the residual generator and MISL-GAN are low enough that visually detectable artifacts and distortion are present. At comparable image qualities, our attack’s performance gains are likely to be significantly more pronounced. Similar results were achieved on the Object Dataset, where our attack generator achieved an ASR that was 4.69% than the residual generator [32] and 12.74% higher than MISL-GAN [30] while maintaining at least 15dB PSNR higher in image quality.

B. Zero-Knowledge Attack Results

Next, we evaluated attack performance in the zero-knowledge scenario, in which the victim CNN is unknown to the attacker and cannot be probed in a black box manner. As a result, the attack’s success relies entirely on transferability.

Table III shows the performance achieved on both datasets by zero-knowledge attacks. Each entry in the table corresponds to the mean attack success rate (ASR) and mean PSNR achieved by an attack when attacking a particular victim CNN detector. The other anti-forensic GANs were omitted from these experiments due to both space limitations, because our anti-forensic generator outperformed these other generators in white-box results presented in Section V-A, and because these generators introduced visible artifacts into attacked images.

Proposed Attack Performance: The results in Table III show that our proposed attack can achieve significant transferability, resulting in strong ASRs even in the zero-knowledge scenario. On the Human Face Dataset, our attack achieved an ASR of 75.10% while maintaining an average PSNR of 40.46. Similarly, our attack achieved an ASR of 70.30% while maintaining an average PSNR of 41.27. These results are particularly important because in many realistic conditions, forensic detectors will be kept private and will not be publicly queryable (e.g. detectors used by governmental and defense agencies, law enforcement, etc.). In these conditions, both white-box and black-box attacks are infeasible.

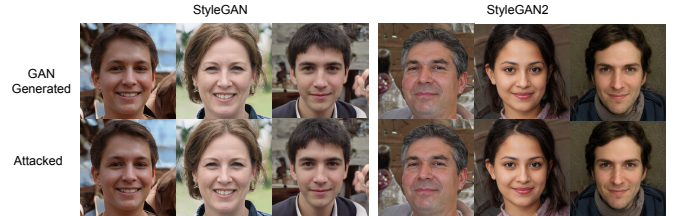


Fig. 3. Attacked images produced by zero-knowledge attack.

Images from the Human Face Dataset attacked using our zero-knowledge attack are shown in Fig. 3. From this figure, we can see that our attack maintains high visual quality without introducing perceptible distortions or artifacts.

We note that when compared to the white-box scenario, the performance drop incurred by our attack in the zero-knowledge scenario was largely attributable to a small number of CNNs. For the Human Face Dataset our attack had lower transferability to both MISLnet and ResNet-50, while on the Object Dataset, our attack had lower transferability to both MISLnet and SRNet. Excluding these CNN, our average ASR is 89.45% on the Human Face Dataset and is 88.20% on the Object Dataset. We note that adversarial example attacks had difficulty attacking these CNNs too. Future studies of this may provide insight into designing CNN architectures that are more resilient to anti-forensic attacks.

Comparison with Adversarial Example Attacks: The zero-knowledge performance of the CW, FGSM and PGD adversarial example attacks are also shown in Table III. To measure the transferability of an adversarial example attack against a particular victim CNN detector, we launched the attack against every other CNN detectors, then used the victim CNN detector to classify the attacked images. For a fair comparison, we chose the parameters for each adversarial example attack such that the mean PSNRs of attacked images were comparable to PSNRs achieved by our attack.

From Table III, we can see that adversarial example attacks were broadly unsuccessful on the Human Face Dataset. The most successful attack was the CW attack, achieving an ASR of 9.97%. Adversarial example attacks were more successful on the Object Dataset, but still achieved ASRs significantly lower than our proposed attack.

VI. CONCLUSION

In this paper, we proposed a new attack to fool GAN-generated image detectors. Our attack uses an adversarially trained generator to synthesize forensic traces that these detectors associate with ‘real’ images. We proposed training protocols to produce both white-box as well as zero-knowledge attacks. The latter protocol, which is based on training against an ensemble of classifiers, enables our attack to achieve transferability to unseen victim classifiers. Through a series of experiments, we demonstrated that our attack does not create perceptible distortions in attacked images, and can fool eight different GAN-generated image detectors. Furthermore, the proposed attack outperforms other alternative attacks in both white-box and zero-knowledge scenarios.

REFERENCES

- [1] I. Goodfellow, J. Pouget-Abadie, M. Mirza, B. Xu, D. Warde-Farley, S. Ozair, A. Courville, and Y. Bengio, "Generative adversarial nets," in *Advances in neural information processing systems*, 2014, pp. 2672–2680.
- [2] Y. Choi, Y. Uh, J. Yoo, and J.-W. Ha, "Stargan v2: Diverse image synthesis for multiple domains," in *Proceedings of the IEEE Conference on Computer Vision and Pattern Recognition*, 2020.
- [3] T. Karras, S. Laine, M. Aittala, J. Hellsten, J. Lehtinen, and T. Aila, "Analyzing and improving the image quality of StyleGAN," in *Proc. CVPR*, 2020.
- [4] T. Karras, S. Laine, and T. Aila, "A style-based generator architecture for generative adversarial networks," in *Proceedings of the IEEE/CVF Conference on Computer Vision and Pattern Recognition*, 2019, pp. 4401–4410.
- [5] A. Brock, J. Donahue, and K. Simonyan, "Large scale gan training for high fidelity natural image synthesis," *arXiv preprint arXiv:1809.11096*, 2018.
- [6] T. Park, M.-Y. Liu, T.-C. Wang, and J.-Y. Zhu, "Gaugan: semantic image synthesis with spatially adaptive normalization," in *ACM SIGGRAPH 2019 Real-Time Live!*, 2019, pp. 1–1.
- [7] T. Karras, T. Aila, S. Laine, and J. Lehtinen, "Progressive growing of gans for improved quality, stability, and variation," *arXiv preprint arXiv:1710.10196*, 2017.
- [8] Y. Choi, M. Choi, M. Kim, J.-W. Ha, S. Kim, and J. Choo, "Stargan: Unified generative adversarial networks for multi-domain image-to-image translation," in *Proceedings of the IEEE Conference on Computer Vision and Pattern Recognition*, 2018.
- [9] D. Cozzolino, J. Thies, A. Rössler, C. Riess, M. Nießner, and L. Verdoliva, "Forensicttransfer: Weakly-supervised domain adaptation for forgery detection," *arXiv preprint arXiv:1812.02510*, 2018.
- [10] S. McCloskey and M. Albright, "Detecting gan-generated imagery using color cues," *arXiv preprint arXiv:1812.08247*, 2018.
- [11] L. Nataraj, T. M. Mohammed, B. Manjunath, S. Chandrasekaran, A. Flenner, J. H. Bappy, and A. K. Roy-Chowdhury, "Detecting gan generated fake images using co-occurrence matrices," *Electronic Imaging*, vol. 2019, no. 5, pp. 532–1, 2019.
- [12] X. Zhang, S. Karaman, and S.-F. Chang, "Detecting and simulating artifacts in gan fake images," in *2019 IEEE International Workshop on Information Forensics and Security (WIFS)*. IEEE, 2019, pp. 1–6.
- [13] S.-Y. Wang, O. Wang, R. Zhang, A. Owens, and A. A. Efros, "Cnn-generated images are surprisingly easy to spot... for now," in *Proceedings of the IEEE/CVF Conference on Computer Vision and Pattern Recognition*, 2020, pp. 8695–8704.
- [14] F. Marra, D. Gragnaniello, L. Verdoliva, and G. Poggi, "Do gans leave artificial fingerprints?" in *2019 IEEE Conference on Multimedia Information Processing and Retrieval (MIPR)*, 2019, pp. 506–511.
- [15] F. Marra, C. Saltori, G. Boato, and L. Verdoliva, "Incremental learning for the detection and classification of gan-generated images," in *2019 IEEE International Workshop on Information Forensics and Security (WIFS)*, 2019, pp. 1–6.
- [16] N. Yu, L. Davis, and M. Fritz, "Attributing fake images to gans: Learning and analyzing gan fingerprints," in *2019 IEEE/CVF International Conference on Computer Vision (ICCV)*, 2019, pp. 7555–7565.
- [17] C. Szegedy, W. Zaremba, I. Sutskever, J. Bruna, D. Erhan, I. Goodfellow, and R. Fergus, "Intriguing properties of neural networks," 2014.
- [18] I. J. Goodfellow, J. Shlens, and C. Szegedy, "Explaining and harnessing adversarial examples," *arXiv preprint arXiv:1412.6572*, 2014.
- [19] A. Kurakin, I. Goodfellow, S. Bengio *et al.*, "Adversarial examples in the physical world," 2016.
- [20] N. Papernot, P. McDaniel, S. Jha, M. Fredrikson, Z. B. Celik, and A. Swami, "The limitations of deep learning in adversarial settings," in *2016 IEEE European symposium on security and privacy (EuroS&P)*. IEEE, 2016, pp. 372–387.
- [21] N. Carlini and D. Wagner, "Towards evaluating the robustness of neural networks," in *2017 IEEE Symposium on Security and Privacy*, May 2017, pp. 39–57.
- [22] A. Madry, A. Makelov, L. Schmidt, D. Tsipras, and A. Vladu, "Towards deep learning models resistant to adversarial attacks," *arXiv preprint arXiv:1706.06083*, 2017.
- [23] M. Barni, M. C. Stamm, and B. Tondi, "Adversarial multimedia forensics: Overview and challenges ahead," in *2018 26th European Signal Processing Conference (EUSIPCO)*. IEEE, 2018, pp. 962–966.
- [24] N. Carlini and H. Farid, "Evading deepfake-image detectors with white- and black-box attacks," in *Proceedings of the IEEE/CVF Conference on Computer Vision and Pattern Recognition Workshops*, 2020, pp. 658–659.
- [25] D. Guera, Y. Wang, L. Bondi, P. Bestagini, S. Tubaro, and E. J. Delp, "A counter-forensic method for cnn-based camera model identification," in *Computer Vision and Pattern Recognition Workshops (CVPRW)*. IEEE, July 2017, pp. 1840–1847.
- [26] M. Barni, K. Kallas, E. Nowroozi, and B. Tondi, "On the transferability of adversarial examples against cnn-based image forensics," *2019 IEEE International Conference on Acoustics, Speech and Signal Processing*, pp. 8286–8290, 2019.
- [27] X. Zhao and M. C. Stamm, "The effect of class definitions on the transferability of adversarial attacks against forensic cnns," *Electronic Imaging*, vol. 2020, no. 4, pp. 119–1, 2020.
- [28] F. Marra, D. Gragnaniello, D. Cozzolino, and L. Verdoliva, "Detection of gan-generated fake images over social networks," in *2018 IEEE Conference on Multimedia Information Processing and Retrieval (MIPR)*, 2018, pp. 384–389.
- [29] X. Yuan, P. He, Q. Zhu, and X. Li, "Adversarial examples: Attacks and defenses for deep learning," *IEEE transactions on neural networks and learning systems*, vol. 30, no. 9, pp. 2805–2824, 2019.
- [30] C. Chen, X. Zhao, and M. C. Stamm, "Mislgan: an anti-forensic camera model falsification framework using a generative adversarial network," in *2018 25th IEEE International Conference on Image Processing (ICIP)*. IEEE, 2018, pp. 535–539.
- [31] D. Cozzolino, J. Thies, A. Rössler, M. Nießner, and L. Verdoliva, "Spoc: Spoofing camera fingerprints," *arXiv preprint arXiv:1911.12069*, 2019.
- [32] D. Kim, H.-U. Jang, S.-M. Mun, S. Choi, and H.-K. Lee, "Median filtered image restoration and anti-forensics using adversarial networks," *IEEE Signal Processing Letters*, vol. 25, no. 2, pp. 278–282, 2017.
- [33] V. Nair and G. E. Hinton, "Rectified linear units improve restricted boltzmann machines," in *Proceedings of the 27th international conference on machine learning (ICML-10)*, 2010, pp. 807–814.
- [34] N. R. Lab, "Public database of stylegan," <https://github.com/NVlabs/stylegan>, 2019.
- [35] —, "Public database of stylegan2," <https://github.com/NVlabs/stylegan2>, 2019.
- [36] Y. Choi, Y. Uh, J. Yoo, and J.-W. Ha, "Pre-trained stargan-v2," <https://github.com/clovaai/stargan-v2>, 2019.
- [37] F. Yu, A. Seff, Y. Zhang, S. Song, T. Funkhouser, and J. Xiao, "Lsun: Construction of a large-scale image dataset using deep learning with humans in the loop," 2016.
- [38] J.-Y. Zhu, T. Park, P. Isola, and A. A. Efros, "Unpaired image-to-image translation using cycle-consistent adversarial networks," in *Proceedings of the IEEE international conference on computer vision*, 2017, pp. 2223–2232.
- [39] F. Chollet, "Xception: Deep learning with depthwise separable convolutions," in *Proceedings of the IEEE conference on computer vision and pattern recognition*, 2017, pp. 1251–1258.
- [40] K. He, X. Zhang, S. Ren, and J. Sun, "Deep residual learning for image recognition," in *Proceedings of the IEEE Conference on Computer Vision and Pattern Recognition (CVPR)*, June 2016.
- [41] G. Huang, Z. Liu, L. Van Der Maaten, and K. Q. Weinberger, "Densely connected convolutional networks," in *Proceedings of the IEEE conference on computer vision and pattern recognition*, 2017, pp. 4700–4708.
- [42] B. Bayar and M. C. Stamm, "Constrained convolutional neural networks: A new approach towards general purpose image manipulation detection," *IEEE Transactions on Information Forensics and Security*, vol. 13, no. 11, pp. 2691–2706, 2018.
- [43] M. Boroumand and J. Fridrich, "Deep learning for detecting processing history of images," *Electronic Imaging*, vol. 2018, no. 7, pp. 213–1, 2018.
- [44] M. Boroumand, M. Chen, and J. Fridrich, "Deep residual network for steganalysis of digital images," *IEEE Transactions on Information Forensics and Security*, vol. 14, no. 5, pp. 1181–1193, 2018.
- [45] Y. Zhan, Y. Chen, Q. Zhang, and X. Kang, "Image forensics based on transfer learning and convolutional neural network," in *Proceedings of the 5th ACM Workshop on Information Hiding and Multimedia Security*, 2017, pp. 165–170.
- [46] A. Tuama, F. Comby, and M. Chaumont, "Camera model identification with the use of deep convolutional neural networks," in *International Workshop on Information Forensics and Security (WIFS)*. IEEE, Dec 2016, pp. 1–6.

- [47] X. Glorot and Y. Bengio, "Understanding the difficulty of training deep feedforward neural networks," in *Proceedings of the Thirteenth International Conference on Artificial Intelligence and Statistics*, ser. Proceedings of Machine Learning Research, Y. W. Teh and M. Titterton, Eds., vol. 9. Chia Laguna Resort, Sardinia, Italy: PMLR, 13–15 May 2010, pp. 249–256. [Online]. Available: <http://proceedings.mlr.press/v9/glorot10a.html>
- [48] N. Papernot, F. Faghri, N. Carlini, I. Goodfellow, R. Feinman, A. Kurakin, C. Xie, Y. Sharma, T. Brown, A. Roy, A. Matyasko, V. Behzadan, K. Hambarzumyan, Z. Zhang, Y.-L. Juang, Z. Li, R. Sheatsley, A. Garg, J. Uesato, W. Gierke, Y. Dong, D. Berthelot, P. Hendricks, J. Rauber, and R. Long, "Technical report on the clevehans v2.1.0 adversarial examples library," *arXiv preprint arXiv:1610.00768*, 2018.